

Critical transition model of edge shear flow formation

Luis GARCIA¹⁾, José M. DELGADO¹⁾, Benjamin A. CARRERAS²⁾, Iván CALVO³⁾,
M. Angeles PEDROSA³⁾ and Carlos HIDALGO³⁾

¹⁾Universidad Carlos III, 28911 Leganés, Madrid, Spain

²⁾BACV Solutions Inc., Oak Ridge, TN 37830, USA

³⁾Asociación EURATOM-CIEMAT, 28040 Madrid, Spain

October 15, 2007

Recently, the experimental results for the emergence of the plasma shear flow layer in TJ-II have been explained as a second-order phase transition like process by using a simple model of envelope equations for the fluctuation level, the averaged poloidal velocity shear, and the pressure gradient [Phys. Plasmas **13**, 122509 (2006)]. Here, we extend this model by incorporating radial coupling. The model is applied to the study of the turbulence-shear flow interaction when the energy flux is low. Transition dynamics and their concomitant thresholds are examined within the context of this model. The effect of an external torque has also been considered. In particular, we analyze the damping rate of the shear flow once the external torque has been removed.

Keywords: Anomalous transport, Shear flow, Phase transition

1 Introduction

The importance of shear flows in magnetically confined plasmas is widely recognized. This in part due to the role that these flows play in improving confinement by turbulence suppression [1, 2]. A current problem in plasma physics is to understand how shear flows are created and how they interact with turbulence. This is a complex problem that can be approached at different levels, going from direct numerical simulations of the plasma to the development of simplified reduced models. In the present paper we follow the latter approach.

The spontaneous formation of shear flows with non-trivial radial structure is studied. Due to the lack of sufficiently high spatial and temporal resolution, it is difficult to formulate an experimental test that will definitively select the dominant mechanisms responsible for the transition. However recent TJ-II experimental results offer the possibility of improved diagnostics with increased radial resolution during and after the transition [3]. Motivated by this, we investigate in this paper the radial structure of the turbulence and poloidal flow in the context of phase transition models.

When the input power is low, we have a transition from L-mode to a different regime. In this regime, the fluctuation level decreases or increases at a slower rate than the input flux, and shear flow is spontaneously developed. We focus our attention on this transition in our starting model.

The model we use for our study is a modified version of the fluctuation-flow model with radial structure [6]. The fluctuation-flow model consists of three coupled partial differential equations of the reaction-diffusion type with

nonlinear diffusivities for the averaged poloidal velocity shear, the envelope of the turbulence fluctuations level, and the pressure. We include the dependence of the coefficients on the pressure gradient [7]. We have derived an expression for the Reynolds stress term in the averaged poloidal flow equation which conserves angular momentum.

2 Transport model

The model is formulated in terms of three fields: the averaged turbulence fluctuation level $E \equiv \langle (\tilde{n}/n_0)^2 \rangle^{1/2}$, where n_0 is the equilibrium plasma density and \tilde{n} is the fluctuation density; the poloidal flow shear, $\sigma \equiv \partial \langle V_\theta \rangle / \partial r$, where $\langle V_\theta \rangle$ denotes poloidal and toroidal average over a magnetic flux surface; and the averaged pressure, p .

$$\frac{\partial E}{\partial t} = N^{2/3} E - N^{-1/2} E^2 - N^{-1/3} \sigma^2 E + \frac{\partial}{\partial x} \left[(D_1 E + D_0) \frac{\partial E}{\partial x} \right] \quad (1)$$

$$\frac{\partial \sigma}{\partial t} = -\sigma - \alpha_3 \frac{\partial^2}{\partial x^2} (N^{-4/3} E^2 \sigma) - \frac{\partial^2}{\partial x^2} \left[(D_2 N^{-5/3} E^2 + D_3) \frac{\partial^2 \sigma}{\partial x^2} \right] \quad (2)$$

$$\frac{\partial p}{\partial t} = S + \frac{\partial}{\partial x} \left[(D_1 E + D_0) \frac{\partial p}{\partial x} \right], \quad (3)$$

where $N \equiv |\partial p / \partial x|$. This is a one-dimensional model in which quantities are assumed to depend only on a normalized radial coordinate, x . The equations are written in terms of dimensionless variables, and x goes from 0 to 1, which corresponds to the shear layer region at the plasma edge.

The first term in the equation for E represents a pressure driven, linear growth of the fluctuations. The second term on the right-hand side models the saturation of turbulence in absence of shear flow, and the third term models the turbulence suppression by shear flow. Here we assume low energy flux so we can neglect diamagnetic effects. The first term on the right-hand side of equation (2) models the poloidal flow shear damping due to magnetic pumping, while the other two terms are contributions from the Reynolds stress. The second term on the right-hand side of equation (2) is a negative viscosity term and represents the generation of poloidal flow by Reynolds stress, and the third term is a hyperdiffusivity and damps the poloidal flow.

We include the dependence of the coefficients on the pressure gradient as in Ref. [7]. Because of the bad magnetic field line curvature at the stellarator edge, we assume that the basic instability underlying the turbulence at the edge of TJ-II is the resistive interchange mode. From the dependence of the coefficients on the linear growth rate, γ , and mode width, W_k , we can derive the dependence of the coefficients on the pressure gradient. We assume that all other dependencies are weak and we take the coefficients to depend only on N . The expression for Reynolds stress contributions is derived by a quasi-linear calculation similar to the one proposed in Ref. [8] and has two terms. The one responsible for the generation of flow is a negative viscosity term and the other is a hyper-viscosity term. The Reynolds stress contributions to the poloidal shear flow equation conserve angular momentum.

The terms involving spatial derivatives are diffusion terms. In equations (1) and (3) these terms have the standard Fick's Law structure, with D_0 representing the collisional diffusion and D_1E representing a renormalized turbulent diffusion. The structure of the negative diffusion operator in equation (2) is due to the fact that in an equation for the shear, the derivative of the momentum. Hyper-diffusivity, with fourth order in the derivative of the shear, keeps a relation two in the orders of source/diffusion derivatives.

We assume that the energy source term $S(x)$ is zero in this layer and that the system is driven by an energy flux Γ_0 from the core, which determines the boundary condition at $x = 0$ according to:

$$\Gamma_0 = -(D_1E + D_0) \frac{\partial p}{\partial x} \Big|_0, \quad p(1) = 0 \quad (4)$$

For the other equations we use zero derivative boundary conditions.

3 Analytic and numerical solutions

For stationary solutions, Eq. (3) is readily integrated, giving a relation between $E(x)$ and $N(x)$,

$$(D_1E + D_0)N = \Gamma_0 \quad (5)$$

Apart from the trivial solution, $E = \sigma = 0$, Equations (1) and (2) have one fixed point solution with $\sigma = 0$, $E = E_0$, and $N = N_0$. From Eq. (1),

$$E_0 = N_0^{7/6} \quad (6)$$

By substitution of Eq. (6) in the relation (5), we obtain the (constant) density gradient for the fixed point solution,

$$D_1N_0^{13/6} + D_0N_0 - \Gamma_0 = 0. \quad (7)$$

For solutions close to the fixed point is possible to derive a simplified description of the system using a multiple scale perturbation analysis. As a first step, we introduce a small parameter δ representing the size of the perturbation, and consider the following expansion

$$\sigma = \delta\sigma_1, \quad E = E_0 + \delta^2E_2, \quad N = N_0 + \delta^2N_2 \quad (8)$$

By substituting the expansion in Eq. (2), and taking into account Eq. (6), we get at first order

$$\frac{\partial\sigma_1}{\partial t} = -\sigma_1 - \alpha_3N_0 \frac{\partial^2\sigma_1}{\partial x^2} - (D_2N_0^{2/3} + D_3) \frac{\partial^4\sigma_1}{\partial x^4} \quad (9)$$

We try as solutions modes like $\sigma_1 = \sigma_{10} \cos(k\pi x)$ which satisfy the boundary conditions. To study their stability properties, we consider a temporal and spatial dependence like

$$\sigma(x, t) = \delta\sigma_{10}e^{\gamma t} \cos(k\pi x) \quad (10)$$

Then, we get from Eq. (9),

$$\gamma = -1 + \alpha_3N_0(k\pi)^2 - (D_2N_0^{2/3} + D_3)(k\pi)^4 \quad (11)$$

This means that the range of possible unstable modes is given by the relation

$$k_- < k < k_+, \quad (12)$$

where

$$(k_{\pm}\pi)^2 = \frac{\alpha_3N_0 \pm \sqrt{(\alpha_3N_0)^2 - 4(D_2N_0^{2/3} + D_3)}}{2(D_2N_0^{2/3} + D_3)} \quad (13)$$

To have instability, there should be an integer k between k_- and k_+ . This gives us a critical value for N , N_c , and, consequently, a threshold value for the flux, Γ_c .

By applying Eq. (13) to different k -values, we can obtain the threshold for Γ_c . We have done a scan in D_2 with k going from 1 to 7 (Fig. 1), the rest of parameters being

$$D_0 = 10^{-3}, \quad D_1 = 10^{-2}, \quad D_3 = 10^{-6}, \quad \alpha_3 = 0.0175$$

We look now for stationary solutions with a given k -value, that is, with the poloidal flow shear at lowest order given by $\sigma(x) = \sigma_{10} \cos(k\pi x)$. From the stability properties of Eq. (2), the stationary solution is the fixed

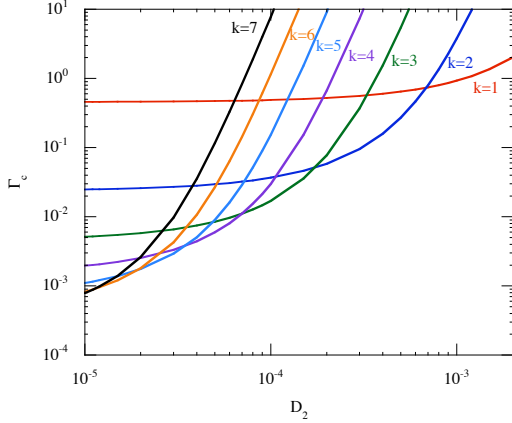


Fig. 1 Flux threshold vs. D_2 for different k -values. The rest of parameters are given in the text.

point solution (7) for values of the flux below Γ_c . Since $\sigma^2 = \sigma_{10}^2 [1 + \cos(2k\pi x)]/2$, we get from Eqs. (1) and (5) that at first order, $E(x) = E_s + E_{21} \cos(2k\pi x)$, and $N(x) = N_s + N_{21} \cos(2k\pi x)$ for values of the flux above Γ_c . By substituting these expansions in Eqs. (2) and (5), and taking into account that $D_0 \ll D_1 E$, and $D_3 \ll D_2 N^{-5/3} E^2$ for the parameters we are using, we get the following expressions,

$$E_s = E_c \left(\frac{\Gamma_0}{\Gamma_c} \right)^{\frac{2}{5}}, \quad (14)$$

$$N_s = \frac{\Gamma_c}{D_1 E_c} \left(\frac{\Gamma_0}{\Gamma_c} \right)^{\frac{3}{5}}, \quad (15)$$

$$\sigma_{10}^2 = 2 \left[\frac{\Gamma_c}{D_1 E_c} \left(\frac{\Gamma_0}{\Gamma_c} \right)^{\frac{3}{5}} - E_c^{\frac{7}{6}} \left(\frac{\Gamma_c}{D_1} \right)^{-\frac{1}{6}} \left(\frac{\Gamma_0}{\Gamma_c} \right)^{\frac{3}{10}} \right] \quad (16)$$

where

$$E_c = (k\pi)^{-\frac{3}{5}} \left(\frac{\Gamma_c}{D_1} \right)^{\frac{2}{5}} \left[\alpha_3 - D_2 (k\pi)^2 \left(\frac{\Gamma_c}{D_1} \right)^{-\frac{2}{13}} \right]^{-\frac{3}{10}} \quad (17)$$

This gives a good approximation to the numerical results for Γ_0 close to the threshold. Since the experimental profiles of the shear flow and fluctuations close the shear layer have few oscillations, we will concentrate in values of the parameter space such as the most unstable modes are $k = 1$ or 2 . In Fig. 2 we compare the analytical and numerical results for $D_2 = 1.5 \times 10^{-3}$ and $k = 1$. The flux threshold for these parameters is 1.358. The analytical results are obtained from Eq. (16), and the numerical results are obtained by advancing numerically Eqs. (1) to (3) until a stationary solution is reached.

4 External torque

To study the effect of an external torque, we add a term $\tau = \tau_0 \cos(k\pi x)$, to the r.h.s. of Eq. (2), so the Equation for

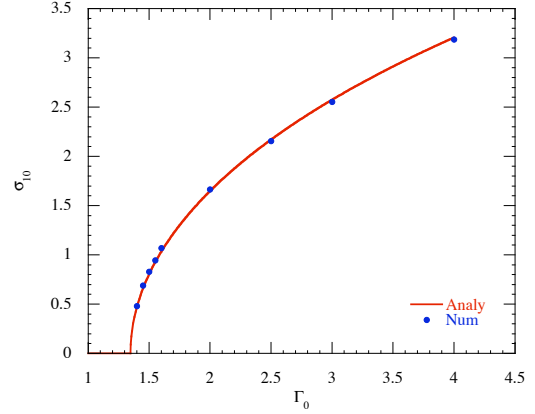


Fig. 2 Comparison of analytical (solid line) and numerical (dots) values of the shear flow for $D_2 = 1.5 \times 10^{-3}$ and $k = 1$.

the shear flow is now

$$\frac{\partial \sigma}{\partial t} = \tau_0 \cos(k\pi x) - \sigma - \alpha_3 \frac{\partial^2}{\partial x^2} (N^{-4/3} E^2 \sigma) - \frac{\partial^2}{\partial x^2} \left[(D_2 N^{-5/3} E^2 + D_3) \frac{\partial^2 \sigma}{\partial x^2} \right] \quad (18)$$

In the rest of the calculations of this paper, we apply the torque during a time $t = 10$, and then we remove the torque to analyze the decay of the shear flow. The evolution of the integral of σ^2 for different values of τ_0 when $\Gamma_0 = 1$ is shown in Fig. 3. For this scan, $D_2 = 1.5 \times 10^{-3}$, and $k = 1$, so we are below the threshold flux in absence of external torque (subcritical regime). In most of the cases the shear flow has two decay scales and the change between them is more pronounced as τ_0 increases. The square root of the integral of σ^2 decays like $e^{\gamma_1 t}$ just after removing the external torque (first decay region), and like $e^{\gamma_2 t}$ at larger times (second decay region). The first decay rate is easily understood from Eq. (18). As we remove the torque, the instantaneous exponential decay rate will be $\gamma_1 = -\tau_0/\sigma_1$, where σ_1 corresponds to the stationary state with external torque τ_0 . The second exponential decay rate is very similar for all the cases, with γ_2 -values between -0.16 and -0.18 .

The evolution of the integral of σ^2 when $\Gamma_0 = 1.35$ is shown in Fig. 4. This value of Γ_0 is very close to the critical value, $\Gamma_c = 1.35794$. For this scan, the evolution of the integral of σ^2 when we suppress the external torque is no longer exponential, and can be fitted to the algebraic expression $C/(1 + t/T)$, where C is a constant (value of the integral when we suppress the external torque), and we take as origin of t the time when we remove the external torque. This is due to the fact that we are approaching the critical point.

We have tried also scans in τ_0 with values of Γ_0 above the threshold (supercritical regime), in particular $\Gamma_0 = 1.37$ and 1.5 . For these cases, the evolution of the integral of σ^2 when we suppress the external torque can be fitted to

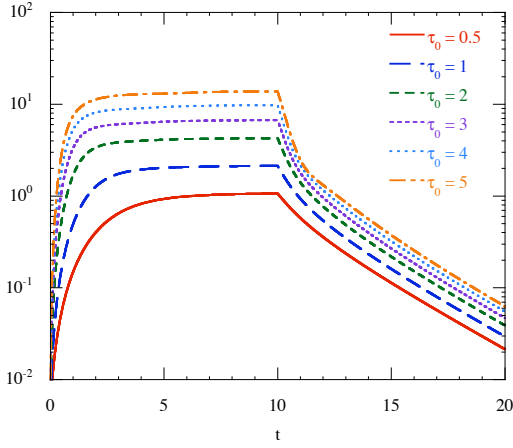


Fig. 3 Evolution of the integral of σ^2 for different values of τ_0 when $\Gamma_0 = 1$. The external torque is suppressed at $t = 10$.

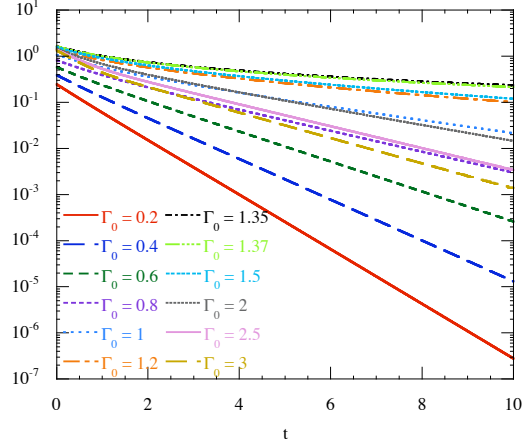


Fig. 5 Evolution of the integral of σ^2 for different values of Γ_0 when $\tau_0 = 0.5$. The origin of t is taken at the time that the external torque is suppressed.

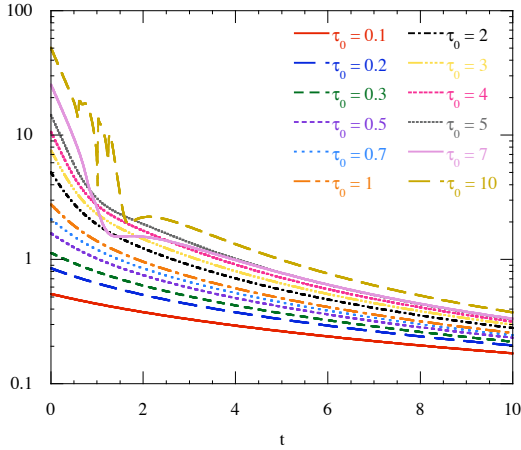


Fig. 4 Evolution of the integral of σ^2 for different values of τ_0 when $\Gamma_0 = 1.35$. The origin of t is taken at the time that the external torque is suppressed.

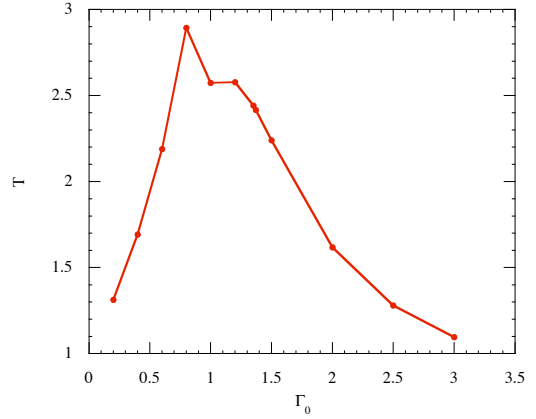


Fig. 6 Results of the exponential fit of the decay of the squared root of the integral of σ^2 for different values of Γ_0 when $\tau_0 = 2$.

$C/(1+t/T) + C_0$, where C_0 is a constant with a value close to the integral of σ^2 for the stationary state in absence of external torque.

Finally, the results for a scan in Γ_0 are shown in Fig. 5. In the y-axis, we represent the integral of σ^2 when we suppress the external torque minus the value for the stationary state in absence of external torque. The slower decay corresponds to the flux value closer to Γ_c , $\Gamma_0 = 1.35$. The decay time tends to infinity as Γ_0 tends to Γ_c , which corresponds to the singularity of the transition point. The data of the evolution of the squared root of the integral of σ^2 for each Γ_0 -value is fitted to $C \exp(-t/T) + C_0$, as it is done in biasing experiments in TJ-II [9]. The results for the decay time T are shown in Fig. 6. The slower decays correspond to flux values closer to Γ_c . The damping is close to the viscous damping (one in our units) only when the flux is far above the threshold. The results are similar when the value of the external torque is changed.

- [1] K. H. Burrell, Phys. Plasmas **4**, 1499 (1997).
- [2] P. W. Terry, Rev. Mod. Phys. **72**, 109 (2000).
- [3] B. Gonçalves, C. Hidalgo, M. A. Pedrosa, R. O. Orozco, E. Sánchez and C. Silva, Phys. Rev. Lett. **96**, 145001 (2006).
- [4] Y. Koide, M. Kikuchi, M. Mori et al., Phys. Rev. Lett. **72**, 3662 (1993).
- [5] K. H. Burrell, M. E. Austin, D. P. Brennan et al., Phys. Plasmas **8**, 2153 (2001).
- [6] D. del-Castillo-Negrete, B. A. Carreras. Physics of Plasmas **9**, 118 (2002).
- [7] B. A. Carreras, L. Garcia, M. A. Pedrosa, C. Hidalgo. Physics of Plasmas **13**, 122509 (2006).
- [8] P. H. Diamond, S.-I. Itoh, K. Itoh, T. S. Hahm, Plasma Phys. Controlled Fusion **47**, R35 (2005).
- [9] M.A. Pedrosa et al., Plasma Phys. Controlled Fusion (2007).